

Fig. S1. MKK4 abundance increases with aging in a panel of tissue biopsies from young and old individual donors. Shown are representative fields of MKK4 immunostaining of lung, small intestine, pancreas, ovary, adrenal gland, stomach, breast, and skin, using tissue arrays. In other tissues (cerebral cortex, cerebellum, muscle, and thymus) MKK4 signals were unchanged.

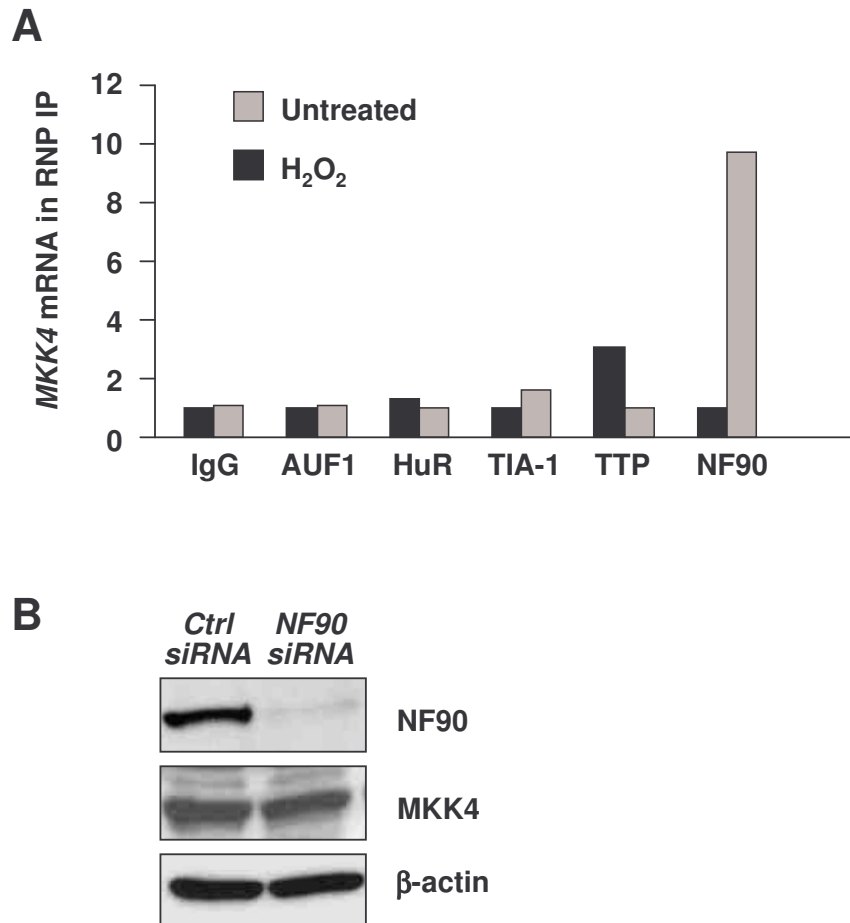


Fig. S2. Survey of putative *MKK4* mRNA-interacting RNA-binding proteins. (A) HeLa whole-cell lysates were used in ribonucleoprotein (RNP) immunoprecipitations (IP) to test the association of *MKK4* mRNA with the RNA-binding proteins (RBPs) HuR, AUF1, TIA-1, TTP, and NF90. RNP associations were tested in lysates prepared from either untreated cells or from cells treated with 1 mM H₂O₂ (in complete medium) and collected 4 hours later. (B) Forty-eight hours after silencing NF90 using specific siRNA, NF90, *MKK4*, and β-actin abundance was measured by Western blot analysis. *MKK4* mRNA appeared to be modestly enriched in TTP IP samples from control cells and was enriched in NF90 IP samples from H₂O₂-treated cells. However, silencing NF90 did not affect *MKK4*, suggesting that NF90 did not modulate *MKK4* abundance. In sum, none of these common RBPs appear to associate with the *MKK4* mRNA or influence *MKK4* abundance.

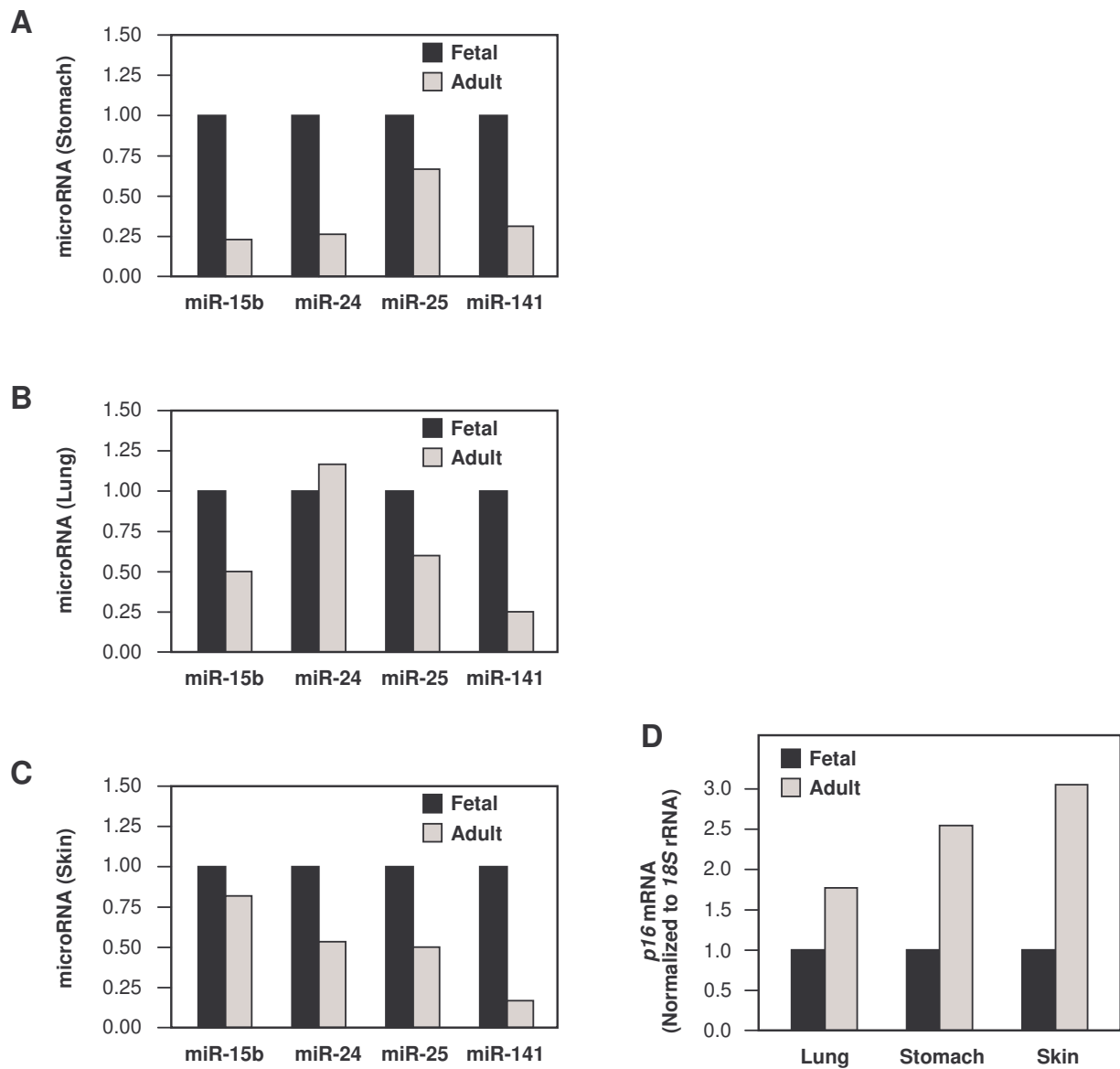
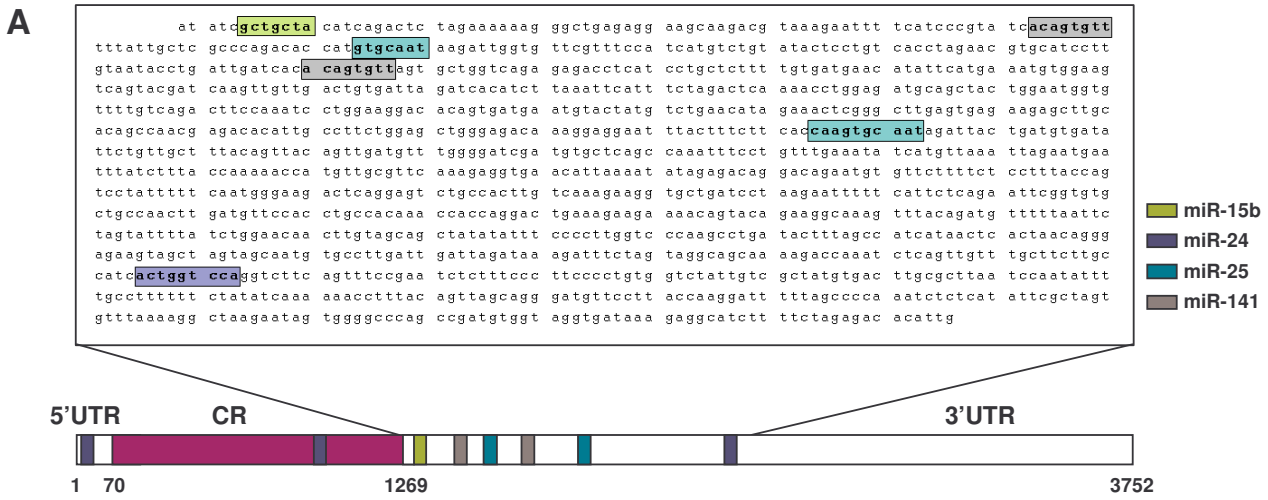
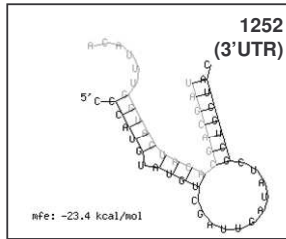


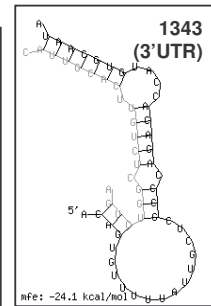
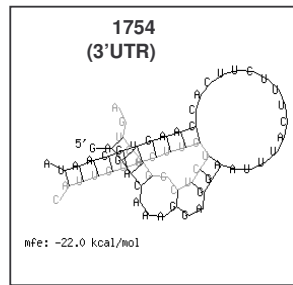
Fig. S3. Higher abundance of predicted human *MKK4* mRNA-directed microRNAs in fetal tissues compared with adult tissues. RNA samples were obtained from stomach (A), lung (B), and skin (C) from fetal or adult donors (Biochain). The abundance of the indicated microRNAs was measured by RT-qPCR and normalized to *U6* (skin) and *18S* rRNA (because *U6* RNA was lower in adult samples than in these two tissues). (D) The abundance of *p16* mRNA (a marker of aging) increased in the adult samples. In A and D, fetal is 40 weeks old and adult is 24 years old. In B and D, fetal is 40 weeks old and adult is 26 years old. In C and D, fetal is 26 weeks old and adult is 83 years old.



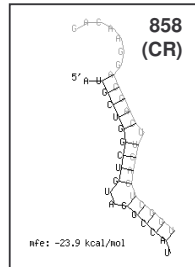
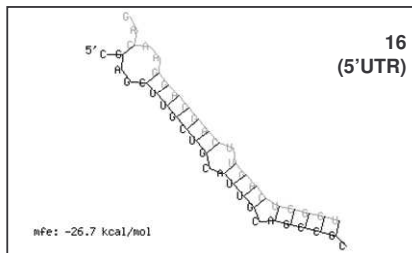
B hsa-miR-15b



hsa-miR-25



hsa-miR-24



hsa-miR-141

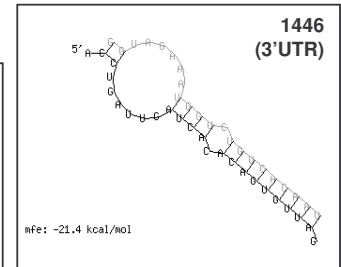
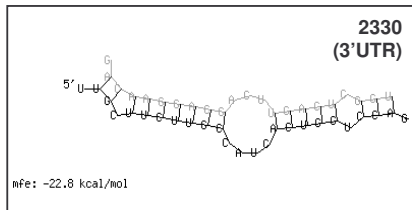
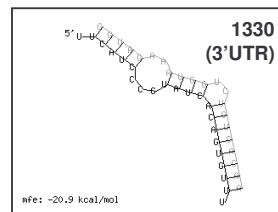


Fig. S4. Predicted microRNA-MKK4 mRNA hybrids. (A) Schematic of the *MKK4* mRNA, including the seed regions of the predicted target sites for miR-15b, miR-24, miR-25, and miR-141. (B) RNA hybrid software (<http://bibiserv.techfak.uni-bielefeld.de/rnahybrid/submission.html>) was used to predict the interaction of *MKK4* and the four miRNAs (miR-15b, miR-24, miR-25, and miR-141). The default stringency settings (including allowance for G:U wobble within the seed region) yielded the predicted sites shown. Except for miR-24, all of the other miRNA-*MKK4* mRNA interactions were also predicted by the more stringent algorithms RNA22, TargetsScan, and Pictar. Gray, miRNA; black, *MKK4* mRNA.

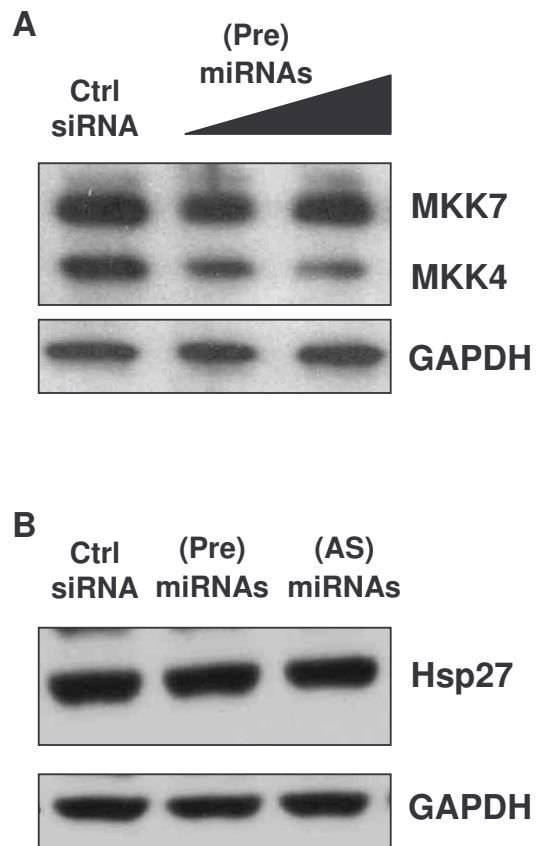


Fig. S5. Unchanged MKK7 and Hsp27 abundance despite changes in MKK4. (A) HeLa cell lysates from cells transfected with either Ctrl siRNA or increasing concentrations (100 and 150 nM) of pooled (Pre)miRNAs were immunoblotted for MKK7, MKK4, and the loading control GAPDH. **(B)** WI-38 cell lysates were prepared 48 hours after transfection with either Ctrl siRNA, (Pre)miRNAs, or (AS)miRNAs. The abundance of Hsp27 and loading control GAPDH was assessed by Western blot analysis.

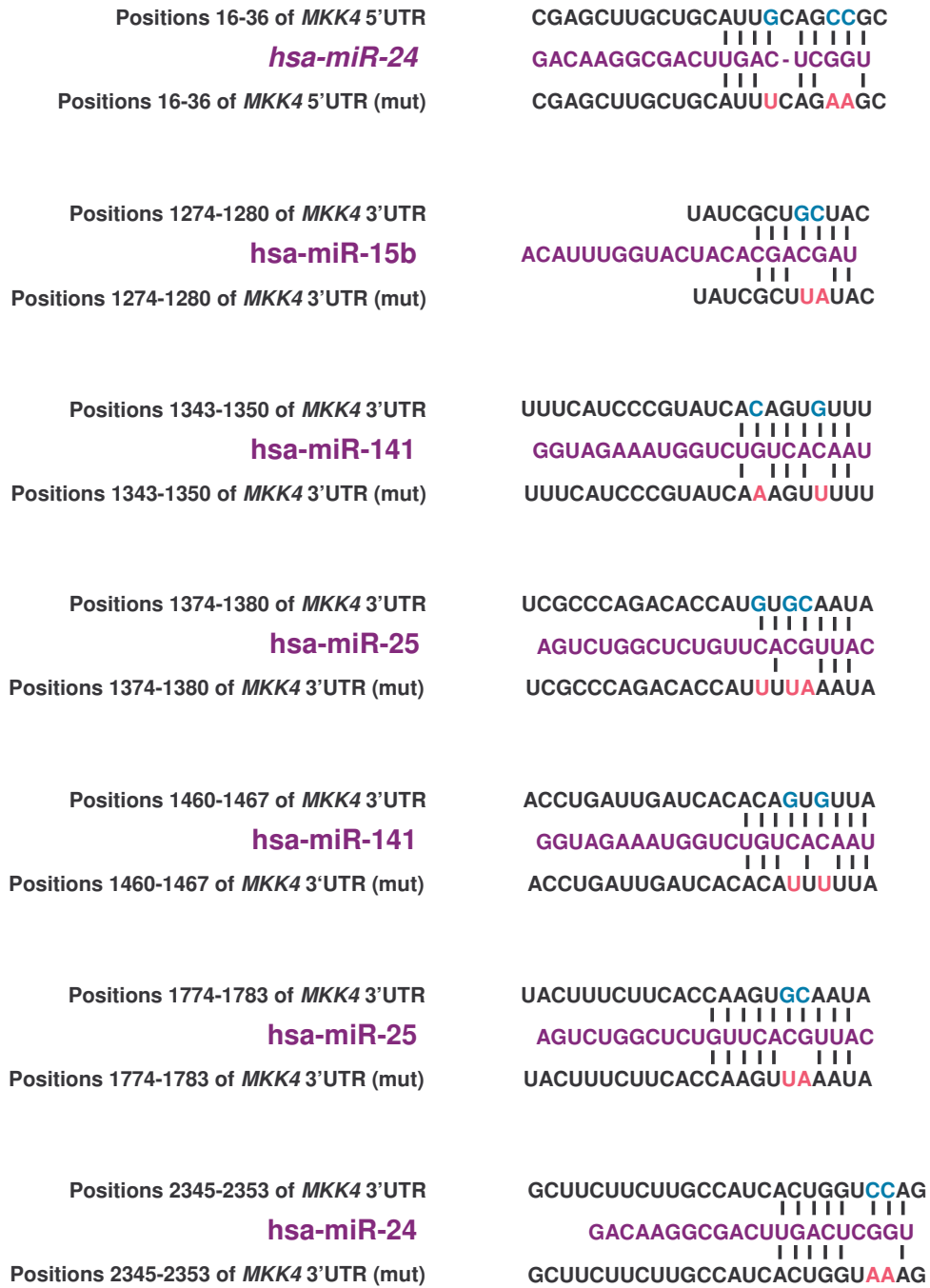


Fig. S6. Point mutations introduced at each predicted microRNA site. Mutated nucleotides (pink) were created by site-directed mutagenesis.

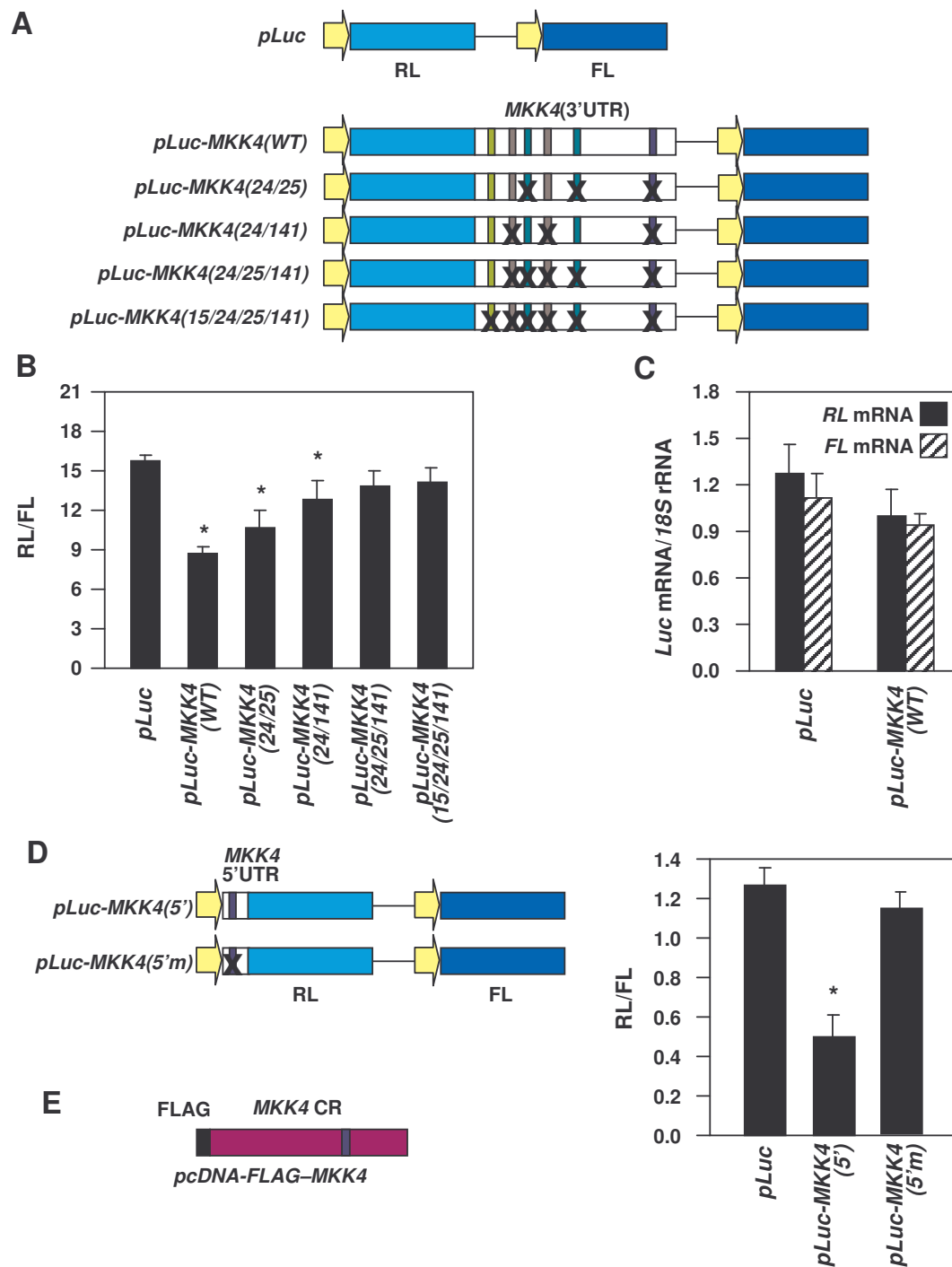


Fig. S7. MKK4 reporter analysis in HeLa cells recapitulates MKK4 reporter analysis in WI-38 HDFs. (A) Schematic representation of the *psiCHECK*TM-2-derived reporter constructs used. *pLuc*, control vector expressing *Renilla* luciferase (RL) and firefly luciferase (FL). *pLuc-MKK4(WT)*, *pLuc* where RL is expressed from a chimeric mRNA bearing the intact 1.3-kb proximal *MKK4* 3'UTR segment bearing all six predicted miRNA sites; *pLuc-MKK4(24/25)* was derived from *pLuc-MKK4(WT)* by introducing mutations (shown as 'X') in the seed regions of miR-24 and miR-25 sites; in *pLuc-MKK4(24/141)*, the mutations were introduced in miR-24 and miR-141 sites; in *pLuc-MKK4(24/25/141)*, the mutations were introduced in miR-24, miR-25, and miR-141 sites; in *pLuc-MKK4(15b/24/25/141)*, all six miRNA sites on the *MKK4* 3' UTR were mutated. **(B)** HeLa cells were transfected with the plasmids shown in (A), and RL activity and (control) FL activity were measured 24 hours later; RL/FL values are shown. **(C)** RL and FL mRNA was measured by RT-qPCR analysis in HeLa cells 24 hours after transfection of *pLuc* and *pLuc-MKK4(WT)*. Data represent the SEM from 3 independent experiments. **(D)** Schematic depicting *pLuc-MKK4(5')* and *pLuc-MKK4(5'm)* which expresses an RL chimeric RNA with the wt and mutated *MKK4* 5'UTR; 24 hours after transfection of *pLuc* (A), *pLuc-MKK4(5')*, and *pLuc-MKK4(5'm)*, RL and FL activities were measured. Data in B to D represent the SEM from 3 independent experiments; *, $p < 0.05$, ANOVA and Tukey multiple comparisons test. **(E)** Schematic depicting plasmid *pcDNA-FLAG-MKK4* and the miR-24 site within the *MKK4* CR.

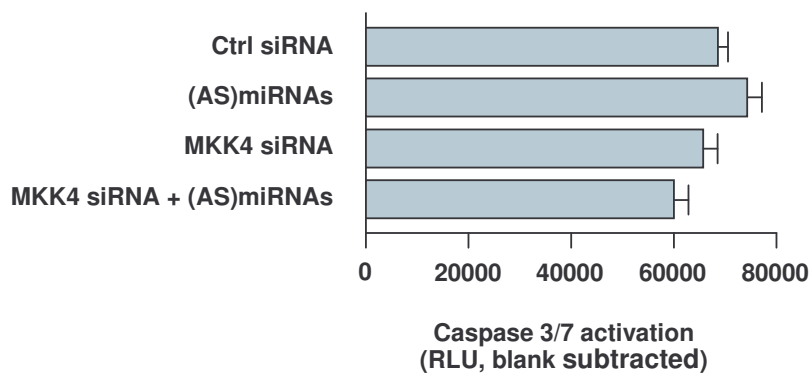


Fig. S8. Activities of caspase-3 and caspase-7 are unaltered after modulating MKK4. WI-38 cells were transfected with Ctrl siRNA, (AS)miRNAs, MKK4 siRNA, or (AS)miRNAs + MKK4 siRNA; 48 hours later, caspase-3 and caspase-7 activities were measured with a Caspase Colorimetric Protease assay kit (Promega, Madison, WI) following the manufacturer's instructions. The values are the SEM from 3 separate experiments. Differences were not significant ($p < 0.05$, ANOVA and Tukey multiple comparisons test).

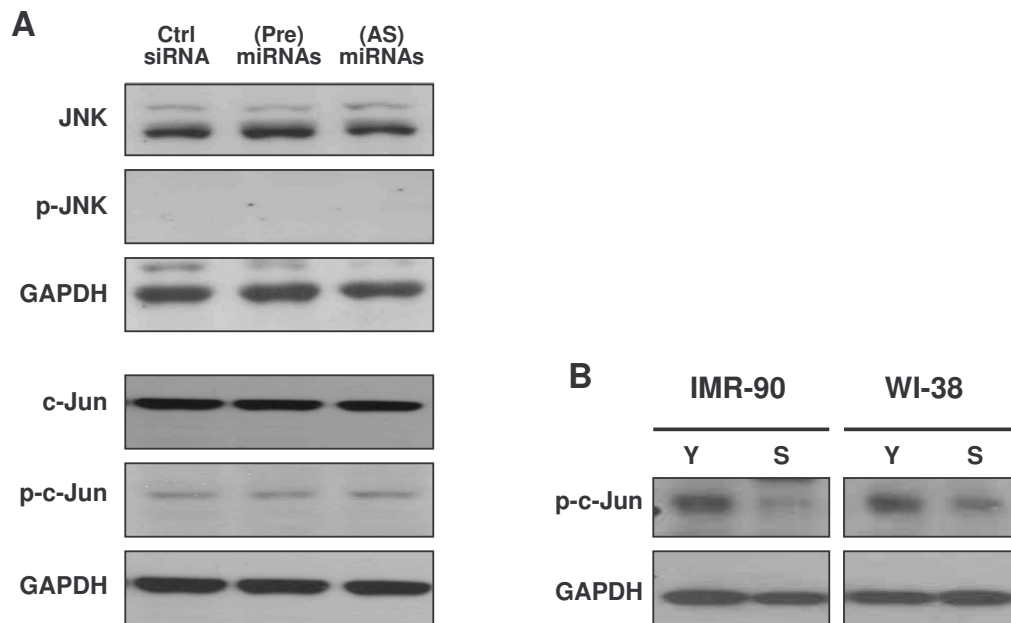


Fig. S9. Analysis of cells treated with (Pre)miRNAs and (AS)miRNAs to modulate MKK4 reveals that MKK4 does not appear to activate the JNK pathway in S cells. (A) WI-38 cells were transfected with Ctrl siRNA, (AS)miRNAs, or (Pre)miRNAs. The amount of total JNK, phospho (p)-JNK, c-Jun (a substrate of JNK), p-c-Jun, as well as GAPDH as a loading control were assessed by Western blot analysis. **(B)** The amounts of p-c-Jun and loading control GAPDH in Y and S fibroblasts were measured by Western blot analysis.